Asian Journal of Andrology (2019) 21, 508–515
www.asiaandro.com; www.ajandrology.com

Open Access

ORIGINAL ARTICLE

Erectile Dysfunction

Human tissue kallikrein-1 protects against the development of erectile dysfunction in a rat model of hyperhomocysteinemia

Kai Cui[1,2,*], Yang Luan[1,2,*], Zhe Tang[1,2], Chuan-Chang Li[1,2], Tao Wang[1,2], Shao-Gang Wang[1,2], Zhong Chen[1,2], Ji-Hong Liu[1,2]

The aim of this study was to investigate the mechanism by which a diet inducing high hyperhomocysteinemia (HHcy) leads to the deterioration of erectile function in rats and whether this is inhibited by expression of the human tissue kallikrein-1 (*hKLK1*) gene. We established a rat model of HHcy by feeding methionine (Met)-rich diets to male Sprague-Dawley (SD) rats. Male wild-type SD rats (WTRs) and transgenic rats harboring the *hKLK1* gene (TGRs) were fed a normal diet until 10 weeks of age. Then, 30 WTRs were randomly divided into three groups as follows: the control (n = 10) group, the low-dose (4% Met, n = 10) group, and the high-dose (7% Met, n = 10) group. Another 10 age-matched TGRs were fed the high-dose diet and designated as the TGR+7% Met group. After 30 days, in all four groups, erectile function was measured and penile tissues were harvested to determine oxidative stress, endothelial cell content, and penis fibrosis. Compared with the 7% Met group, the TGR+7% Met group showed diminished HHcy-induced erectile dysfunction (ED), indicating the improvement caused by hKLK1. Regarding corpus cavernosum endothelial cells, hKLK1 preserved endothelial cell-cell junctions and endothelial cell content, and activated protein kinase B/endothelial nitric oxide synthase (Akt/eNOS) signaling. Fibrosis assessment indicated that hKLK1 preserved normal penis structure by inhibiting apoptosis in the corpus cavernosum smooth muscle cells. Taken together, these findings showed that oxidative stress, impaired corpus cavernosum endothelial cells, and severe penis fibrosis were involved in the induction of ED by HHcy in rats, whereas hKLK1 preserved erectile function by inhibiting these pathophysiological changes.

Asian Journal of Andrology (2019) **21**, 508–515; doi: 10.4103/aja.aja_111_18; published online: 1 January 2019

Keywords: endothelial cell; erectile function; fibrosis; human tissue kallikrein-1; hyperhomocysteinemia; oxidative stress

INTRODUCTION

Recent epidemiologic studies revealed that erectile dysfunction (ED), defined as the inability to attain or maintain enough erection for satisfactory sexual intercourse, has a high incidence and prevalence worldwide, affecting up to 150 million men.[1–3] ED can be induced by many pathological conditions including vascular risk factors or diseases, neurologic abnormalities, and hormonal disturbances.[4,5] Among all such factors, hyperhomocysteinemia (HHcy), characterized by elevation of total plasma homocysteine (tHcy), attracts increasing attention as a novel risk factor for cardiovascular disorders.[6] Numerous studies showed that HHcy perturbs vascular endothelial function.[7,8] Jones *et al*.[8] reported that HHcy markedly inhibited corpus cavernosum (CC) endothelial cells (ECs) function and nitric oxide (NO) formation in animal experiments and proposed HHcy as a newly described potential risk factor for ED. Moreover, some clinical trials indicated that HHcy, known as an important contributor to endothelial dysfunction, is a determinant for ED.[9–11]

Although oral phosphodiesterase (PDE) 5 inhibitors, first-line drugs for ED, are generally effective and well-tolerated therapies,[12–14] they usually have limitations. PDE5 inhibitors cannot increase cyclic guanosine monophosphate (cGMP) levels if the bioavailability of endogenous NO is restricted, as their effects rely on endogenous formed NO. This also explains why these drugs fail to relieve ED in men with severe cardiovascular disease. Therefore, novel treatment methods are urgently needed for patients responding poorly to PDE5 inhibitors.

Tissue kallikrein-1 (KLK1) is a glycoprotein of the serine proteinase superfamily, initially discovered as a hypotensive agent in human urine.[15,16] It processes low-molecular-weight kininogen (LMWK) to produce vasoactive kinins, which exert such biological functions as decreasing cardiac and renal injuries, restenosis, and ischemic stroke, and promoting angiogenesis and skin wound healing, all via kinin receptor signaling.[17] Previous studies in transgenic animals harboring the human tissue *KLK1* (*hKLK1*) gene showed that *KLK1* induced a variety of beneficial biological effects, including increasing endothelial function,[18] anti-apoptosis, anti-fibrosis, and decreasing oxidative stress.[19–21] We showed that hKLK1 play a preventive role in age-related ED in our previous study,[22] and have been studying whether hKLK1 could be used to preserve erectile function in the presence of HHcy.[23,24]

[1]Department of Urology, Tongji Hospital, Tongji Medical College, Huazhong University of Science and Technology, Wuhan 430030, China; [2]Institute of Urology, Tongji Hospital, Tongji Medical College, Huazhong University of Science and Technology, Wuhan 430030, China.
*These authors contributed equally to this work.
Correspondence: Dr. Z Chen (chenzhongtj@126.com) or Dr. JH Liu (jhliu@tjh.tjmu.edu.cn)
Received: 13 April 2018; Accepted: 24 October 2018

We established a rat model of HHcy in male Sprague–Dawley (SD) rats, induced by a methionine (Met)-rich diet. We then examined the effect of HHcy on erectile function and CC in this model. Moreover, whether harboring the *hKLK1* gene could preserve erectile function in the rats with HHcy was also studied. Our results provided an experimental basis for the use of *hKLK1* as an alternative therapy for ED.

MATERIALS AND METHODS

Acquisition of the transgenic rats

As shown in our previous study,[22] we obtained transgenic rats harboring the *hKLK1* gene (TGRs) as a generous gift from the Max Delbrück Center for Molecular Medicine (Berlin, Germany). The TGRs were generated by microinjecting a 5.6-kb DNA fragment containing the entire *hKLK1* gene, under the control of heavy metal-responsive mouse metallothionein promoter, into the oocytes of SD rats. The presence of the transgene in genomic DNA was verified by Southern blot. Offspring with the homozygous *hKLK1* gene were selected for further experiments.

Animals and treatment

This study was approved by the Academic Administration Committee of Tongji Hospital, Tongji Medical College, Huazhong University of Science and Technology (HUST), Wuhan, China. All animal experiments were performed based on the guideline of the Animal Ethical Committee for Animal Experiments in China. A total of 40 male SD rats were used, including 30 wild-type rats (WTRs), obtained from the Laboratory Animal Center of Tongji Medical College (HUST), and 10 TGRs. The 30 WTRs, 10 weeks of age and weighing 300–350 g, were randomly divided into three groups (n = 10 per group): control, low-dose (4% Met), and high-dose (7% Met). The Met enriched diets were fed orally to the rats of 4% Met and 7% Met groups daily for 1 month. The 10 age-matched TGRs, designated as the TGR+7% Met group, were also fed 7% Met diet for a month. All rats were individually housed in a conventional animal facility with laminar flow, maintained at 20°C ± 1°C and 50% ± 10% relative humidity with a 12 h light/12 h dark photoperiod, and bred by professional breeders.

Verification of TGR

Measurements at the levels of genome, genomics transcription and translation were used to detect the presence and expression of the *hKLK1* gene in the CC of rats. The presence of *hKLK1* gene in the genomic DNA obtained from frozen CC samples was detected through conventional polymerase chain reaction (PCR) and agarose gel electrophoresis. The primer sequences are listed in **Supplementary Table 1**. mRNA and protein expressions were assayed by real-time reverse transcriptase-PCR (RT-PCR) and western blot analysis, respectively.

Measurement of erectile function

As reported in our previous studies,[22,25] the rat carotid artery was cannulated (PE-50 tubing; Kindly, Shanghai, China) for continuous measurement of arterial pressure to get the mean arterial pressure (MAP). Then, cavernous nerve was isolated on the posterolateral aspect of the prostate gland, followed by the electrical stimulation with a bipolar electrode at 15 Hz frequency, with a 1.2-ms width for 1 min. A 25G needle (Kindly) was inserted into the right crura to continuously monitor intracavernosal pressure (ICP). All data were recorded by a data acquisition system (PowerLab 4SP; ADInstruments, Dunedin, New Zealand). Erectile response was elicited by electrical field stimulation with 2.5 V and 5 V. The ratios of maximum (max) ICP and the area under the ICP curve (AUC) to MAP were calculated to evaluate penile erectile function.

After the measurement, the middle region of the skin-denuded penile shaft was maintained overnight in 4% paraformaldehyde (Beyotime Biotechnology, Haimen, China) and then embedded in paraffin for histologic studies. The remaining two penile tissues were harvested and stored at −80°C for real-time RT-PCR, western blot, and enzyme-linked immunosorbent assay (ELISA). In addition, these rats' blood samples were obtained from the carotid artery for subsequent experiments.

Determination of antioxidant activity

CC tissues were stored at −80°C until they were assayed for antioxidant activity. Test kits for measuring malondialdehyde (MDA, S0131, Beyotime Biotechnology) and superoxide dismutase (SOD, S0101, Beyotime Biotechnology) were used according to the manufacturer's protocol. Penile MDA levels and SOD activities were normalized to the wet weight of penile tissue samples.

Masson's trichrome staining

CC tissue samples from rats were sectioned transversely (5-μm thickness). Smooth muscle and collagen content were quantitatively analyzed in Masson's trichrome-stained sections, examined at ×100 magnification. The ratios of areas of smooth muscle (red) to areas of collagen (blue) were considered to reflect the tissue fibrosis. These data were calculated using ImagePro Plus software (Media Cybernetics, Silver Spring, MD, USA) in five randomly selected sections per group.

Assessment of apoptosis

Terminal deoxynucleotidyl transferase 2'-deoxyuridine 5'-triphosphate nick end labeling (TUNEL) staining was used to assess apoptosis in the CC. Penile sections were processed in accordance with the instructions of the *In situ* Cell Death Detection Kit (Roche Diagnostic Corporation, Indianapolis, IN, USA). Nuclei were stained with hematoxylin (Beyotime Biotechnology). Five sections per group were randomly selected and assessed at ×400. The apoptosis level was expressed at the ratio of apoptotic to total cells in the CC sections.

Immunohistochemistry

Sections (5-μm thickness) were incubated overnight at 4°C with antibodies against α-smooth muscle actin (α-SMA; 1:100; Abcam, Cambridge, MA, USA). Sections were then washed three times and incubated with a biotinylated secondary antibody (1:1000; Proteintech, Wuhan, China). Finally, antigen-antibody reactions were detected by staining with diaminobenzidine (Beyotime Biotechnology). Semi-quantitative analysis was performed to evaluate staining intensities using ImagePro Plus software.

Immunofluorescence

Sections were processed for immunofluorescence and incubated with the following primary antibodies against platelet/EC adhesion molecule (PECAM)-1 (1:100), endothelial nitric oxide synthase (eNOS; 1:50), and α-SMA (1:100; Abcam). Slides were then washed and incubated with DyLight-conjugated secondary antibodies (1:200, Abbkine, Redlands, CA, USA). Nuclei were stained with 4',6-diamidino-2-phenylindole (DAPI; Beyotime Biotechnology). Fluorescence images were acquired using an Olympus BX51 fluorescence microscope (Olympus Corporation, Tokyo, Japan).

Real-time RT-PCR

Total RNA in the CC samples was extracted using the Multisource Total RNA Minipre Kit (Axygen, Tewsbury, MA, USA) according to

the manufacturer's instructions. Conventional PCR and real-time RT-PCR were performed with the PrimeScript RT Master Mix and SYBR Green PCR Master Mix (TaKaRa, Dalian, China), respectively. Relative values of mRNA expression of targeted genes to that of β-actin were calculated using the $2^{-\Delta CT}$ method. The primer sequences of *hKLK1*, rat tissue *KLK1* (*rKLK1*), and β-actin are listed in **Supplemental Table 1**.

Western blot analysis

CC samples of each group were homogenized in radioimmunoprecipitation assay (RIPA) buffer (Beyotime Biotechnology) containing a protease inhibitor cocktail and phosphatase inhibitor cocktail (Roche Applied Science, Indianapolis, IN, USA). Concentrations of soluble proteins were measured using the bicinchoninic acid assay (Beyotime Biotechnology). Protein samples (40 μg per lane) were separated by sodium dodecyl sulfate-polyacrylamide gel electrophoresis and transferred to polyvinylidene difluoride membranes (Millipore, Darmstadt, Germany). This experiment included primary antibodies against hKLK1 (1:5000; Sigma Aldrich, St. Louis, MO, USA), rKLK1 (1:1000; Sigma Aldrich), p22phox (1:500; Santa Cruz, Dallas, TX, USA), p47phox (1:1000; Sangon Biotech, Shanghai, China), gp91phox (1:500; Proteintech), vascular endothelial (VE)-cadherin (1:1000; Abcam), Occludin (1:1000; Abcam), claudin-5 (1:1000; Abcam), protein kinase B (Akt; 1:1000; Proteintech), phospho-Akt (p-Akt; Ser473, 1:1000; Cell Signaling Technology, Danvers, MA, USA), eNOS (1:500; Abcam), phospho-eNOS (p-eNOS; S1177; 1:500; Cell Signaling Technology), α-SMA (1:1000; Abcam), transforming growth factor-β1 (TGF-β1; 1:1000; Abcam), B-cell lymphoma-2 (Bcl-2, 1:1000; Affinity, Zhenjiang, China), Bcl-2 associated X protein (Bax; 1:500; Proteintech), and β-actin (1:1000; Proteintech). Membranes were then incubated with horseradish peroxidase-conjugated secondary antibodies (1:5000; Proteintech) and analyzed using an enhanced chemiluminescence detection system (Pierce, Thermo Fisher Scientific, Rockford, IL, USA).

Statistical analyses

Results are presented as a mean ± standard deviation. Data were analyzed using one-way analysis of variance followed by Tukey's multiple comparison test to identify differences among multiple groups. The unpaired *t*-test was performed to analyze differences between any two groups and a value of $P < 0.05$ was considered as statistically significant.

RESULTS

Metabolic parameters

There was no obvious difference in initial weight and plasma tHcy levels among the four groups. After 1 month feeding with the Met-rich diet, tHcy levels in rats in the 4% Met, 7% Met, and TGR+7% Met groups were obviously higher than that in the control group fed a standard diet (all $P < 0.05$). Moreover, tHcy levels in the 7% Met and TGR+7% Met groups were higher than that in the 4% Met group (both $P < 0.05$). In addition, final weights in the 4% Met, 7% Met, and TGR+7% Met groups were lower than that in the control group (all $P < 0.05$), and were lower in the 7% Met and TGR+7% Met groups than that in the 4% Met group. Interestingly, there were no differences in tHcy levels or final weights in the 7% Met and TGR+7% Met groups (**Supplementary Table 2**). Together, elevated tHcy levels demonstrated that the rat model for HHcy was successfully established through Met-rich diets, consistent with previous reports.[26,27]

hKLK1 inhibited erectile dysfunction induced by HHcy

Electrostimulation of the rat cavernous nerve with different voltages (2.5 V and 5 V) was performed to evaluate erectile function. Max ICP/MAP ratios in the 4% Met and 7% Met groups were sharply attenuated compared with that in the control group, and the value for the 7% Met group was also lower than for the 4% Met group ($P < 0.05$). However, erectile function was partly improved in the TGR+7% Met group, though it was still lower than that in the control group ($P < 0.05$). The ratios of AUC/MAP at the 2.5 V and 5 V in all four groups showed the same trends as did the max ICP/MAP values. In addition, there were no differences among the four groups in the MAP ($P = 0.9763$; **Figure 1**).

Verification of the hKLK1 gene expression in the CC

The presence and expression of *hKLK1* gene in rat CC samples were verified at the levels of genomic DNA, mRNA, and protein. The results showed that rats in only the TGR+7% Met group contained the *hKLK1* DNA fragments, and there were transcription and translation of fragments to hKLK1 mRNA and protein, respectively. In addition, *rKLK1* expression was lower in the 4% Met and 7% Met groups than that in the control group at both mRNA and protein levels, and its expression in the 7% Met group was also lower than that in the 4% Met group (all $P < 0.05$; **Figure 2**). These data suggested that only the TGRs, not the WTRs, contained and expressed the *hKLK1* gene in the CC.

hKLK1 inhibited oxidative stress in the CC of rats with HHcy

We determined the expression of nicotinamide adenine dinucleotide phosphate-oxidase (NADPH oxidase) subunits including $p22^{phox}$, $p47^{phox}$, and $gp91^{phox}$. These subunits expression levels were higher in the 4% Met and 7% Met groups than that in the control group, and expression in the 7% Met group was higher than that in the 4% Met group. Although there were also differences between the control and TGR+7% Met groups, expression in the TGR+7% Met was much lower than that in the other groups with HHcy. MDA levels and SOD activities, both reflecting oxidative stress, were also tested using ELISA. MDA levels in the four groups showed a similar trend as did expression of NADPH oxidase subunits. SOD activities in the 4% Met and 7% Met groups were lower than that in the control group, and that in the 7% Met group was also lower than that in the 4% Met group. SOD activity in the TGR+7% Met group was slightly higher than that in the 7% Met group (all $P < 0.05$; **Figure 3**).

hKLK1 preserved EC and activated Akt/eNOS pathway in CC of rats with HHcy

We determined roles of ECs and Akt/eNOS pathway in ED induced by HHcy through western blot and immunofluorescence. Expression of EC junction proteins (VE-cadherin, occludin, and claudin-5) was lower in the 4% Met and 7% Met groups than that in the control group. Their expression in the 7% Met group was also lower than that in the 4% Met group, while it was grately elevated in TGR+7% Met group compared with that in the 7% Met group. Moreover, immunofluorescence staining for PECAM-1 and eNOS in cavernous tissues showed a similar trend as did expression of EC junction proteins (all $P < 0.05$; **Figure 4** and **5**). In addition, western blot results of p-Akt, eNOS and p-eNOS/eNOS ratio showed similar results (all $P < 0.05$); however, there were no differences in Akt expression among all the four groups ($P = 0.3065$; **Figure 5**).

hKLK1 inhibited fibrosis and apoptosis in the CC of rats with HHcy

By Masson's trichrome staining, the area ratios of smooth muscle cells (SMC; red) to collagen (blue) in the 4% Met and 7% Met groups were lower than that in the control group, indicating more fibrosis, and the ratio for the 7% Met group was also lower than that for the 4% Met group. The TGR+7% Met group showed less histologic changes compared with the 7% Met group, in the rats with HHcy. α-SMA

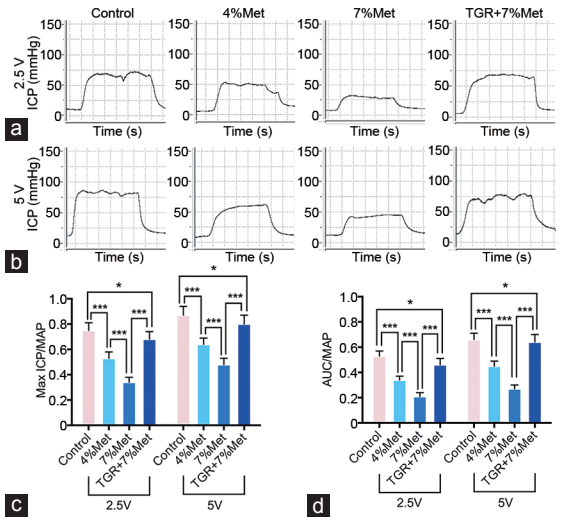

Figure 1: Erectile function of rats elicited by cavernous nerve electrical stimulation. Representative ICP curves through electrostimulation of (**a**) 2.5 V and (**b**) 5 V for 1 min, respectively. Ratios of both max ICP and AUC to MAP of all four groups were presented through bar graphs: (**c**) for max ICP/MAP, and (**d**) for AUC/MAP. Data are expressed as mean ± standard deviation ($n = 10$ per group). $^{*}P < 0.05$, $^{***}P < 0.001$. Met: methionine; TGR: transgenic rats; ICP: intracavernous pressure; AUC: area under the curve; MAP: mean arterial pressure.

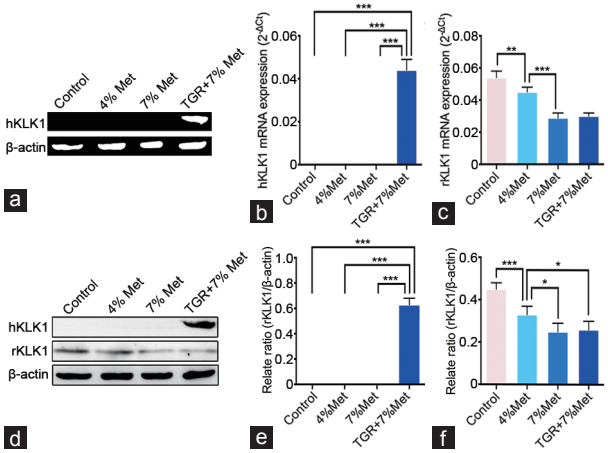

Figure 2: Verification of the existence and expression of *hKLK1* gene in CC of rats. (**a**) Representative *hKLK1* genomic DNA bands in CC through conventional polymerase chain reaction followed by agarose gel electrophoresis. Relative mRNA expression of *hKLK1* and *rKLK1* genes to β-actin in CC of all four groups by real-time reverse transcriptase polymerase chain reaction: (**b**) for *hKLK1* and (**c**) for *rKLK1*. (**d**) Representative western blot result of hKLK1 and rKLK1 proteins in CC of rats. Western blot results were presented through bar graphs with β-actin as the loading control: (**e**) for hKLK1 and (**f**) for rKLK1. Data are shown as mean ± standard deviation ($n = 10$ per group). $^{*}P < 0.05$, $^{**}P < 0.01$ and $^{***}P < 0.001$. Met: ethionine; TGR: transgenic rats; CC: corpus cavernosum; *hKLK1*: human tissue kallikrein-1; *rKLK1*: rat tissue kallikrein-1.

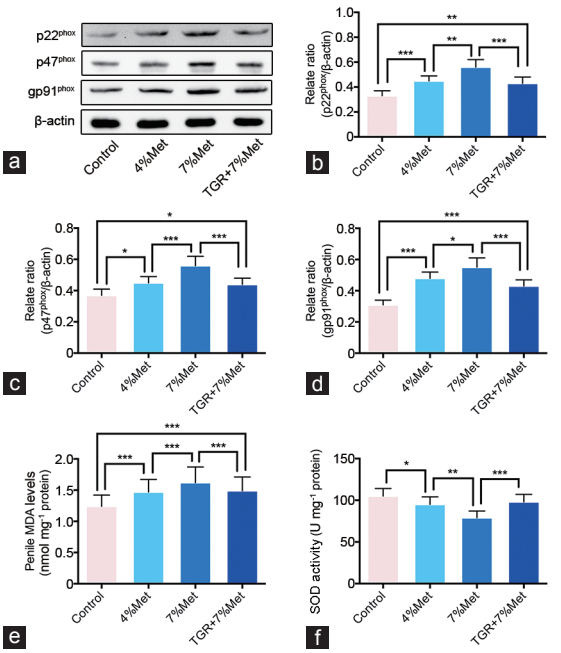

Figure 3: hKLK1 could inhibit oxidative stress in CC of rats with HHcy. (**a**) Representative western blot results of $p22^{phox}$, $p47^{phox}$ and $gp91^{phox}$ in CC of rats. Expressions of $p22^{phox}$, $p47^{phox}$ and $gp91^{phox}$ with β-actin as the loading control in all four groups were presented through bar graphs: (**b**) for $p22^{phox}$, (**c**) for $p47^{phox}$ and (**d**) for $gp91^{phox}$. (**e**) MDA levels determined by the ELISA method in all four groups. (**f**) SOD activities determined by the ELISA method in all four groups. Data are expressed as mean ± standard deviation ($n = 5$ per group). $^{*}P < 0.05$, $^{**}P < 0.01$ and $^{***}P < 0.001$. Met: methionine; hKLK1: human tissue kallikrein-1; CC: corpus cavernosum; HHcy: hyperhomocysteinemia; TGR: transgenic rats; ELISA: enzyme linked immunosorbent assay; SOD: superoxide dismutase.

expression in the four groups, as indicated by immunohistochemistry, immunofluorescence and western blot, showed the same trend as the SMC area in Masson's trichrome staining. Western blot also showed enhanced expression of TGF-β1 in 4% Met and 7% Met groups compared with that in the control group, and was higher in the 7% Met than in the 4% Met group. The TGR+7% Met group had lower TGF-β1 expression than the 7% Met group did (all $P < 0.05$; **Figure 6**). In addition, the apoptosis index by TUNEL staining and the Bax/Bcl-2 ratio by western blot showed the same trend in the four groups as did the TGF-β1 (all $P < 0.05$; **Supplementary Figure 1**).

DISCUSSION

This study is the first to describe a protective role of hKLK1 on erectile function of rats with HHcy, using the TGR model. Our data suggested that HHcy-induced ED was accompanied by oxidative stress, impaired ECs and severe fibrosis in the CC. However, enhancing the kallikrein-kinin system (KKS) through harboring the *hKLK1* gene could inhibit oxidative stress, protect the eNOS pathway, maintain the normal histologic structure of the CC, and thus, preserve erectile function in rats with HHcy.

Regarding the link between HHcy and ED, Khan *et al.*[28] reported that Hcy plays a negative role in endothelium-dependent relaxation and NO formation in the rabbit CC and that this effect was potentiated by copper and reversed by SOD or catalase. Similarly, a previous study showed elevated plasma Hcy levels were strongly correlated with the occurrence of ED.[9] This was consistent with our findings that high tHcy levels and impaired erectile function occurred in the rats with HHcy, and that harboring the *hKLK1* gene preserved erectile function in these animals. Moreover, we observed weight loss in the rats with HHcy, which was also reported in a previous study.[26] This weight loss might be associated with a metabolic disorder induced by HHcy, supporting our findings on *rKLK1*.[29] Chaussalet *et al.*[30] showed increased expression of hKLK1 in human ECs exposed to Hcy. However, endothelium was not the only source of overall KLK1 expression in our experiment because the protein expressed in other cells of the CC besides ECs.

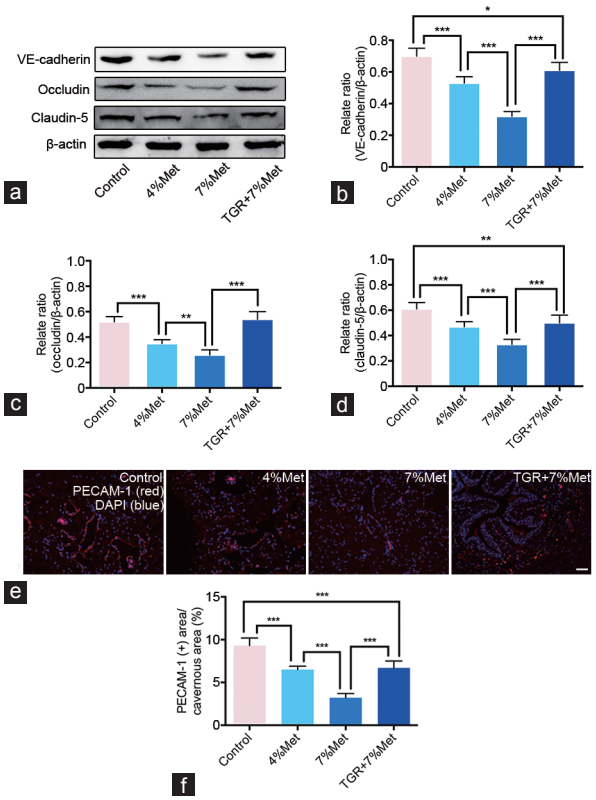

Figure 4: hKLK1 could preserve EC junction protein expressions and endothelial content in CC of rats with HHcy. (**a**) Representative western blot results for VE-cadherin, occludin and claudin-5 in CC of rats of all four groups. Expressions of VE-cadherin, occludin and claudin-5 with β-actin as the loading control in all four groups were presented through bar graphs: (**b**) for VE-cadherin, (**c**) for occluding, and (**d**) for claudin-5. (**e**) Immunofluorescence results of PECAM-1 in rats of all four groups. (**f**) Ratios of PECAM-1 positive area to cavernous area were presented through bar graphs. Data are expressed as mean ± standard deviation (n = 5 per group). $^{*}P < 0.05$, $^{**}P < 0.01$ and $^{***}P < 0.001$. Scale bars = 100 μm. Met: methionine; hKLK1: human tissue kallikrein-1; CC: corpus cavernosum; HHcy: hyperhomocysteinemia; TGR: transgenic rats; PECAM-1: platelet/endothelial cell adhesion molecule-1; EC: endothelial cell.

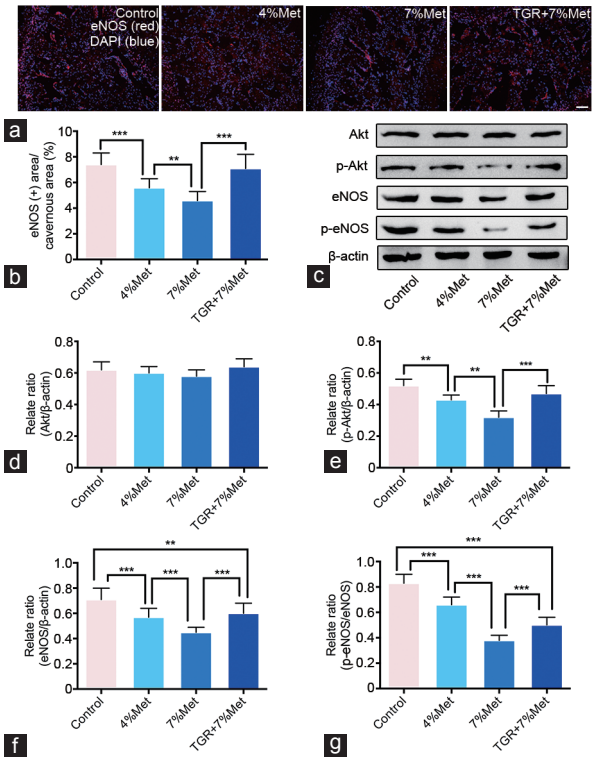

Figure 5: hKLK1 activates Akt/eNOS signaling pathway in CC of rats with HHcy. (**a**) Immunofluorescence results of eNOS in CC of rats of all four groups. (**b**) Ratios of eNOS positive area to cavernous area were presented through bar graphs. (**c**) Representative western blot results for Akt, p-Akt, eNOS and p-eNOS in rats of all four groups. Expressions of Akt, p-Akt and eNOS with β-actin as the loading control in all four groups were presented through bar graphs: (**d**) for Akt, (**e**) for p-Akt and (**f**) for eNOS. (**g**) The ratio of p-eNOS/eNOS was presented through bar graph. Data are expressed as mean ± standard deviation (n = 5 per group). $^{**}P < 0.01$, and $^{***}P < 0.001$. Scale bars = 100 μm. Met: methionine; hKLK1: human tissue kallikrein-1; CC: corpus cavernosum; HHcy: hyperhomocysteinemia; TGR: transgenic rats; Akt: protein kinase B; eNOS: endothelial nitric oxide synthase.

Study on ED induced by diabetes showed a close association between ED and reactive oxygen species (ROS).[31] ROS are generated by NADPH oxidase, xanthine oxidase, NOS, cyclooxygenase, and lipoxygenase. NADPH oxidase, a multi-subunit enzyme, including $p47^{phox}$, $p67^{phox}$, $gp91^{phox}$, $p22^{phox}$, and $p40^{phox}$, is considered as a major source of ROS formation in the penis. Excessive ROS in penile tissue was reported to attenuate NO bioavailability and promote apoptosis of CC SMCs, thus leading to ED.[32] Similarly, we previously reported S-allyl cysteine supplementation restored erectile function in diabetic rats by preventing ROS formation through inhibition of NADPH oxidase subunit expression.[33] In addition, we also found some NADPH oxidase subunits were greatly activated in the CC of rats with androgen deficiency.[34] A recent study by Jiang *et al.*[26] also reported oxidative stress contributed to ED induced by HHcy. Our data on NADPH oxidase subunit expression, MDA levels, and SOD activities verified the existence of oxidative stress in rats with HHcy. These effects were substantially diminished by hKLK1, demonstrating the anti-oxidation effect of hKLK1 in rats with HHcy.

Oxidative stress is considered to impair functions of normal ECs.[35] ECs adhere to one another by a complex network of transmembrane adhesive proteins.[36] These endothelial intercellular junctional proteins comprise tight junctions and adhere junctions. Tight junctions regulate paracellular permeability, while adhere junctions are crucial for EC growth.[36,37] It was reported that downregulation of the representative tight junction proteins (occludin and claudin-5) and a representative adhere junction protein (VE-cadherin) in the CC was involved in the deterioration of erectile function induced by hypercholesterolemia[27] and diabetes.[32] In our study, levels of endothelial intercellular junctional proteins in the four groups suggested that these junctions were impaired in the CC of rats with HHcy and that harboring the *hKLK1* gene preserved their expression. In addition to endothelial intercellular junctions, EC content is also crucial.[38] PECAM-1 is a transmembrane immunoglobulin concentrated at intercellular contacts in the endothelium and is used as an EC marker. Its expression in our study indicated that a loss of ECs was involved in ED induced by HHcy, a finding consistent with previous studies in diabetic and hypercholesterolemia animals.[27,32] However, harboring the *hKLK1* gene preserved the EC content in the CC of rats with HHcy. Taken together, our results indicated that impaired endothelial intercellular junctional proteins and EC content were both factors involved in HHcy-induced ED, and, furthermore, that hKLK1 was protective.

NO is generated by three different isoforms of NOS: eNOS, neuronal NOS (nNOS), and inducible NOS (iNOS). Among these,

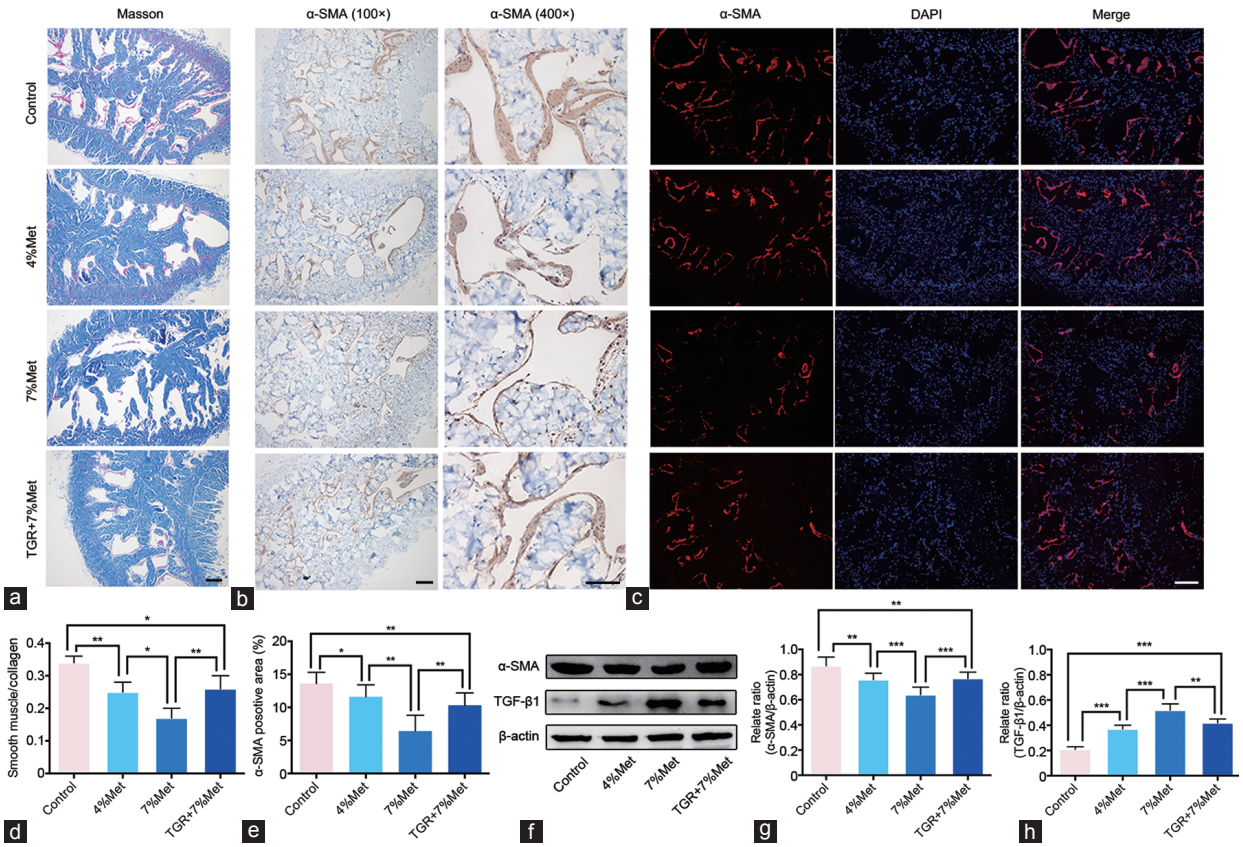

Figure 6: hKLK1 could reduce fibrosis in CC of rats with HHcy. (**a**) Masson's trichrome staining results of CC of rats in all four groups. (**b**) Immunohistochemical staining result of α-SMA in CC of rats (×100 and ×400). (**c**) Immunofluorescence results of α-SMA in CC of rats. (**d**) Ratios of smooth muscle to collagen were presented through bar graphs. (**e**) Ratios of α-SMA positive area to cavernous area were presented through bar graphs. (**f**) Representative western blot results for α-SMA and TGF-β1 in CC of rats. Expressions of α-SMA and TGF-β1 with β-actin as the loading control in all four groups were presented through bar graphs: (**d**) for α-SMA and (**e**) for TGF-β1. Data are expressed as mean ± standard deviation (n = 5 per group). $^{*}P < 0.05$, $^{**}P < 0.01$ and $^{***}P < 0.001$. All scale bars = 100 μm. Met: methionine; hKLK1: human tissue kallikrein-1; CC: corpus cavernosum; HHcy: hyperhomocysteinemia; TGR: transgenic rats; α-SMA: α-smooth muscle actin; TGF-β1: transforming growth factor-β1.

eNOS is an important factor in ED.[39,40] In previous studies, eNOS activity was inhibited during ED induced by hypercholesterolemia,[27] diabetic,[32,41] advanced age,[22] and HHcy.[26] Moreover, a low eNOS activity in the CC was also characterized by decreased eNOS phosphorylation level at the Ser1177 site under aging[22] and diabetic[41] conditions. We found eNOS phosphorylation and the Akt/eNOS pathway were inhibited under HHcy conditions, and that, in rats harboring the *hKLK1* gene, eNOS phosphorylation level and the Akt/eNOS pathway activity were increased.

Although ECs are believed to be associated with the ability to achieve normal penile corporal veno-occlusion, CC SMC content is another important factor. The decrease of CC SMCs content, excessive collagen deposition, and a corresponding decreased ratio of smooth muscle to collagen in the CC were all associated with age-related ED in both human and rat.[42,43] Moreover, fibrosis, emerged as the predominant underlying cause of ED, is also evident in various rat models, including diabetes, hyperlipidemia, and androgen deficiency.[44–46] Our study found the decrease of CC SMCs, the excessive collagen deposition, and a corresponding decrease in the ratio of SMC to collagen in the CC of rats with HHcy. However, *hKLK1* gene could attenuate these pathological changes and maintain normal CC structure in rats with HHcy.

To explore why HHcy decreased the number of CC SMCs, we analyzed the apoptosis level in CC SMCs. Apoptosis is an important mechanism of cellular self-destruction and is considered to be closely associated with fibrosis. Zhang *et al.*[47] reported that apoptosis was significant during fibrosis, and that decreasing apoptosis alleviated fibrosis in diabetic rats. Furthermore, Wang *et al.*[48] found that androgen deficiency caused corporal fibrosis by promoting CC SMCs apoptosis in rats. We found that apoptosis levels were increased under the HHcy condition and that the *hKLK1* gene inhibited HHcy-induced apoptosis in the TGRs. This result was consistent with our previous report that hKLK1 inhibited apoptosis in the CC of aged rats.[22]

Although our study elucidated several mechanisms of ED induction by HHcy, its major limitation was the absence of cell-based experiments. Moreover, the absence of total *KLK1* (human and rat) measurements was another limitation. Therefore, in future studies, we will isolate ECs and SMCs from the CC of rats and verify the effect of hKLK1 *in vitro* to further support our findings.

CONCLUSIONS

This study revealed that oxidative stress, dysregulated cavernous ECs, and severe penis fibrosis were involved in ED induced by HHcy in rats, while hKLK1 preserved erectile function through inhibition of these pathophysiological changes. Thus, hKLK1 is promising as a potential preventive factor for ED induced by HHcy because of its numerous beneficial effects.

AUTHOR CONTRIBUTIONS

KC and YL participated in the design of the trial, conducted the data acquisition, interpreted and analyzed the data, and drafted and revised the manuscript. ZT, CCL, and TW designed the study and contributed to the study materials. SGW pointed out deficiencies and ameliorated the manuscript. JHL and ZC guided the experiment directions and drafted the manuscript. All authors read and approved the final manuscript.

COMPETING INTERESTS

All authors declare no competing interests.

ACKNOWLEDGMENTS

This work was supported by a grant from the National Natural Science Foundations of China (No. 81270690 and No. 81372759).

Supplementary Information is linked to the online version of the paper on the *Asian Journal of Andrology* website.

REFERENCES

1 Platek AE, Hrynkiewicz-Szymanska A, Kotkowski M, Szymanski FM, Syska-Suminska J, *et al*. Prevalence of erectile dysfunction in atrial fibrillation patients: a cross-sectional, epidemiological study. *Pacing Clin Electrophysiol* 2016; 39: 28–35.
2 Landripet I, Stulhofer A. Is pornography use associated with sexual difficulties and dysfunctions among younger heterosexual men? *J Sex Med* 2015; 12: 1136–9.
3 Capogrosso P, Colicchia M, Ventimiglia E, Castagna G, Clementi MC, *et al*. One patient out of four with newly diagnosed erectile dysfunction is a young man – worrisome picture from the everyday clinical practice. *J Sex Med* 2013; 10: 1833–41.
4 Friedewald VE, Kornman KS, Beck JD, Genco R, Goldfine A, *et al*. The American Journal of Cardiology and Journal of Periodontology Editors' Consensus: periodontitis and atherosclerotic cardiovascular disease. *Am J Cardiol* 2009; 104: 59–68.
5 Shamloul R, Ghanem H. Erectile dysfunction. *Lancet* 2013; 381: 153–65.
6 Selhub J. Homocysteine metabolism. *Annu Rev Nutr* 1999; 19: 217–46.
7 Gurda D, Handschuh L, Kotkowiak W, Jakubowski H. Homocysteine thiolactone and N-homocysteinylated protein induce pro-atherogenic changes in gene expression in human vascular endothelial cells. *Amino Acids* 2015; 47: 1319–39.
8 Jones RW, Jeremy JY, Koupparis A, Persad R, Shukla N. Cavernosal dysfunction in a rabbit model of hyperhomocysteinaemia. *BJU Int* 2005; 95: 125–30.
9 Demir T, Comlekci A, Demir O, Gulcu A, Calypkan S, *et al*. Hyperhomocysteinemia: a novel risk factor for erectile dysfunction. *Metabolism* 2006; 55: 1564–8.
10 Al-Hunayan A, Thalib L, Kehinde EO, Asfar S. Hyperhomocysteinemia is a risk factor for erectile dysfunction in men with adult-onset diabetes mellitus. *Urology* 2008; 71: 897–900.
11 Demir T, Cömlekci A, Demir O, Gülcü A, Calıskan S, *et al*. A possible new risk factor in diabetic patients with erectile dysfunction: homocysteinemia. *J Diabetes Complications* 2008; 22: 395–9.
12 Goldstein I, Lue TF, Padma-Nathan H, Rosen RC, Steers WD, *et al*. Oral sildenafil in the treatment of erectile dysfunction. Sildenafil Study Group. *N Engl J Med* 1998; 338: 1397–404.
13 Porst H, Rosen R, Padma-Nathan H, Goldstein I, Giuliano F, *et al*. The efficacy and tolerability of vardenafil, a new, oral, selective phosphodiesterase type 5 inhibitor, in patients with erectile dysfunction: the first at-home clinical trial. *Int J Impot Res* 2001; 13: 192–9.
14 Brock GB, McMahon CG, Chen KK, Costigan T, Shen W, *et al*. Efficacy and safety of tadalafil for the treatment of erectile dysfunction: results of integrated analyses. *J Urol* 2002; 168: 1332–6.
15 Wang J, Xiong W, Yang Z, Davis T, Dewey MJ, *et al*. Human tissue kallikrein induces hypotension in transgenic mice. *Hypertension* 1994; 23: 236–43.
16 Bhoola KD, Figueroa CD, Worthy K. Bioregulation of kinins: kallikreins, kininogens, and kininases. *Pharmacol Rev* 1992; 44: 1–80.
17 Chao J, Shen B, Gao L, Xia CF, Bledsoe G, *et al*. Tissue kallikrein in cardiovascular, cerebrovascular and renal diseases and skin wound healing. *Biol Chem* 2010; 391: 345–55.
18 Fu SS, Li FJ, Wang YY, You AB, Qie YL, *et al*. Kallikrein gene-modified EPCs induce angiogenesis in rats with ischemic hindlimb and correlate with integrin alphavbeta3 expression. *PLoS One* 2013; 8: e73035.
19 Gao L, Bledsoe G, Yin H, Shen B, Chao L, *et al*. Tissue kallikrein-modified mesenchymal stem cells provide enhanced protection against ischemic cardiac injury after myocardial infarction. *Circ J* 2013; 77: 2134–44.
20 Mohanraj R, Silva JA, Santana ET, Manchini MT, Antônio EL, *et al*. Exercise training can prevent cardiac hypertrophy induced by sympathetic hyperactivity with modulation of kallikrein-kinin pathway and angiogenesis. *PLoS One* 2014; 9: e91017.
21 Aburto A, Barria A, Cardenas A, Carpio D, Figueroa CD, *et al*. Pre-stimulation of the kallikrein system in cisplatin-induced acute renal injury: an approach to renoprotection. *Toxicol Appl Pharmacol* 2014; 280: 216–23.
22 Luan Y, Ruan Y, Wang T, Zhuan L, Wen Z, *et al*. Preserved erectile function in the aged transgenic rat harboring human tissue kallikrein 1. *J Sex Med* 2016; 13: 1311–22.
23 Cui K, Tang Z, Luan Y, Rao K, Wang T, *et al*. Preserved erectile function in the hyperhomocysteinaemia transgenic rat harboring human tissue kallikrein 1. *Eur Urol Suppl* 2017; 16: e1953.
24 Cui K, Tang Z, Luan Y, Rao K, Wang T, *et al*. Preserved erectile function in the hyperhomocysteinaemia transgenic rats harboring human tissue kallikrein. *Transl Androl Urol* 2017; 6: AB087.
25 Cui K, Luan Y, Wang T, Zhuan L, Rao K, *et al*. Reduced corporal fibrosis to protect erectile function by inhibiting the Rho-kinase/LIM-kinase/cofilin pathway in the aged transgenic rat harboring human tissue kallikrein 1. *Asian J Androl* 2017; 19: 67–72.
26 Jiang W, Xiong L, Bin Y, Li W, Zhang J, *et al*. Hyperhomocysteinaemia in rats is associated with erectile dysfunction by impairing endothelial nitric oxide synthase activity. *Sci Rep* 2016; 6: 26647.
27 Ryu JK, Kim WJ, Koh YJ, Piao S, Jin HR, *et al*. Designed angiopoietin-1 variant, COMP-angiopoietin-1, rescues erectile function through healthy cavernous angiogenesis in a hypercholesterolemic mouse. *Sci Rep* 2015; 5: 9222.
28 Khan MA, Thompson CS, Emsley AM, Mumtaz FH, Mikhailidis DP, *et al*. The interaction of homocysteine and copper markedly inhibits the relaxation of rabbit corpus cavernosum: new risk factors for angiopathic erectile dysfunction? *BJU Int* 1999; 84: 720–4.
29 Ebbesen LS, Olesen SH, Kruhoffer M, Ingerslev J, Orntoft TF. Folate deficiency induced hyperhomocysteinemia changes the expression of thrombosis-related genes. *Blood Coagul Fibrinolysis* 2006; 17: 293–301.
30 Chaussalet M, Lamy E, Foucault-Bertaud A, Genovesio C, Sabatier F, *et al*. Homocysteine modulates the proteolytic potential of human vascular endothelial cells. *Biochem Biophys Res Commun* 2004; 316: 170–6.
31 Malavige LS, Levy JC. Erectile dysfunction in diabetes mellitus. *J Sex Med* 2009; 6: 1232–47.
32 Jin HR, Kim WJ, Song JS, Piao S, Choi MJ, *et al*. Intracavernous delivery of adesigned angiopoietin-1 variant rescues erectile function by enhancingendothelial regeneration in the streptozotocin-induced diabetic mouse. *Diabetes* 2011; 60: 969–80.
33 Yang J, Wang T, Yang J, Rao K, Zhan Y, *et al*. S-allyl cysteine restores erectile function through inhibition of reactive oxygen species generation in diabetic rats. *Andrology* 2013; 1: 487–94.
34 Li R, Meng X, Zhang Y, Wang T, Yang J, *et al*. Testosterone improves erectile function through inhibition of reactive oxygen species generation in castrated rats. *PeerJ* 2016; 4: e2000.
35 Griendling KK, Sorescu D, Ushio-Fukai M. NAD(P)H oxidase: role in cardiovascular biology and disease. *Circ Res* 2000; 86: 494–501.
36 Dejana E. Endothelial cell-cell junctions: happy together. *Nat Rev Mol Cell Biol* 2004; 5: 261–70.
37 Yan HH, Mruk DD, Cheng CY. Junction restructuring and spermatogenesis: the biology, regulation, and implication in male contraceptive development. *Curr Top Dev Biol* 2007; 80: 57–92.
38 Ryu JK, Zhang LW, Jin HR, Piao S, Choi MJ, *et al*. Derangements in endothelial cell-to-cell junctions involved in the pathogenesis of hypercholesterolemia-induced erectile dysfunction. *J Sex Med* 2009; 6: 1893–907.
39 Aversa A, Bruzziches R, Francomano D, Natali M, Gareri P, *et al*. Endothelial dysfunction and erectile dysfunction in the aging man. *Int J Urol* 2010; 17: 38–47.
40 Chiou WF, Liu HK, Juan CW. Abnormal protein expression in the corpus cavernosum impairs erectile function in type 2 diabetes. *BJU Int* 2010; 105: 674–80.
41 Cui K, Ruan Y, Wang T, Rao K, Chen Z, *et al*. FTY720 supplementation partially improves erectile dysfunction in rats with streptozotocin-induced type 1 diabetes through inhibition of endothelial dysfunction and corporal fibrosis. *J Sex Med* 2017; 14: 323–35.
42 Bakircioglu ME, Sievert KD, Nunes L, Lau A, Lin CS, *et al*. Decreased trabecular smooth muscle and caveolin-1 expression in the penile tissue of aged rats. *J Urol* 2001; 166: 734–8.
43 Melman A, Gingell JC. The epidemiology and pathophysiology of erectile dysfunction. *J Urol* 1999; 161: 5–11.
44 Ruan Y, Li M, Wang T, Yang J, Rao K, *et al*. Taurine supplementation improves erectile function in rats with streptozotocin-induced type 1 diabetes via amelioration of penile fibrosis and endothelial dysfunction. *J Sex Med* 2016; 13: 778–85.
45 Li R, Cui K, Wang T, Wang S, Li X, *et al*. Hyperlipidemia impairs erectile function in rats by causing cavernosal fibrosis. *Andrologia* 2017; 49. Doi: 10.1111/and.12693. [Epub Ahead of Print].
46 Cui K, Li R, Chen R, Li M, Wang T, *et al*. Androgen deficiency impairs erectile function in rats through promotion of corporal fibrosis. *Andrologia* 2018; 50. doi: 10.1111/and.12797. [Epub Ahead of Print].

47 Zhang L, Ding WY, Wang ZH, Tang MX, Wang F, *et al*. Early administration of trimetazidine attenuates diabetic cardiomyopathy in rats by alleviating fibrosis, reducing apoptosis and enhancing autophagy. *J Transl Med* 2016; 14: 109.
48 Wang XJ, Xu TY, Xia LL, Zhong S, Zhang XH, *et al*. Castration impairs erectile organ structure and function by inhibiting autophagy and promoting apoptosis of corpus cavernosum smooth muscle cells in rats. *Int Urol Nephrol* 2015; 47: 1105–15.

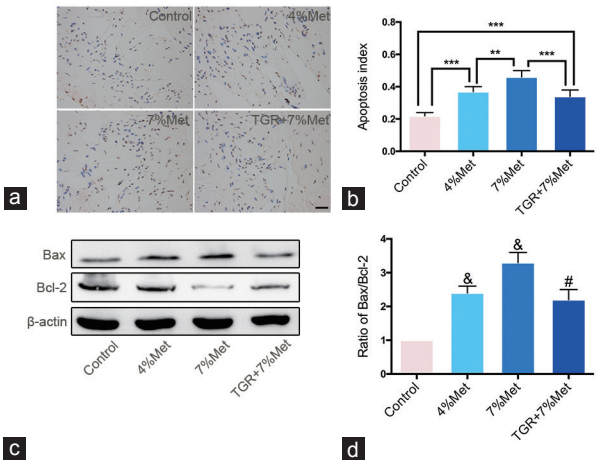

Supplementary Figure 1: hKLK1 could reduce apoptosis in CC of rats with HHcy. (**a**) Apoptosis levels in all four groups was determined by TUNEL method. (**b**) Apoptosis index was presented through bar graph. (**c**) Representative western blot results for Bax and Bcl-2 in CC of rats. (**d**) Ratios of Bax to Bcl-2 with β-actin as the loading control in all four groups were presented through bar graphs. Data are expressed as mean ± standard deviation (n = 5 for per group). $^{**}P < 0.01$, $^{***}P < 0.001$. $^{\&}P < 0.05$ when compared with the control group, and $^{\#}P < 0.05$ when compared with the 7% Met group; Scale bar = 100 μm. Met: methionine; hKLK1: human tissue kallikrein-1; CC: corpus cavernosum; HHcy: hyperhomocysteinemia; TGR: transgenic rats; TUNEL: terminal deoxynucleotidyl transferase 2'-deoxyuridine 5'-triphosphate nick end labeling.

Supplementary Table 1: Primers used in conventional polymerase chain reaction and real-time reverse transcriptase-polymerase chain reaction

Genes	*Primer sequences*	*Usage (PCR)*
hKLK1	F: 5'-GTCCAGAAGGTGACAGACTTCAT-3' R: 5'-GTCCTCGATCCACTTCACATAAG-3' F: 5'-CTCACAGCTGCTCATTGCATC-3' R: 5'-GCTCTCACTGACATGAACAAACTGG-3'	Conventional Real-time
rKLK1	F: 5'-CCCACACACAGATGGTGACAGA-3' R: 5'-CCTTGAAGCACACCATCACAGAG-3'	Real-time
β-actin	F: 5'- AAGAGCTATGAGCTGCCTGA-3' R: 5'- TACGGATGTCAACGTCACAC-3'	Conventional and real-time

RT-PCR: reverse transcriptase-polymerase chain reaction; *hKLK1*: human tissue kallikrein-1; *rKLK1*: rat tissue kallikrein-1

Supplementary Table 2: Metabolic parameters

Variable	*Control*	*4% Met*	*7% Met*	*TGR+7% Met*
Initial weight (g)	307.5±8.9	309.43±11.3	306.15±13.41	310.74±9.53
Final weight (g)	415.41±21.33	366.27±27.34*	342.53±22.82*	350.48±19.98*
Initial tHcy level (μmol l^{-1})	30.23±4.94	31.72±5.25	30.47±4.33	29.92±4.74
Final tHcy level (μmol l^{-1})	31.22±5.75	84.49±15.88*	110.77±25.28*	105.84±17.75*
MAP	97.17±11.03	98.73±10.11	100.08±9.37	98.43±8.41

Data are shown as mean±s.d.; $^{*}P<0.05$ when compared with the control group. Met: methionine; TGR: transgenic rat; tHcy: total plasma homocysteine; MAP: mean atrial pressure; s.d.: standard deviation